NAZARBAYEV UNIVERSITY

SCHOOL OF MEDICINE

Master thesis

TITLE: Investigating autophagy as a potential pathway of anticancer mechanism of Phenformin

Student: Kamila Khikhmetova, ORCID ID 0009-0003-0911-9876

Program: Master of Pharmacology and Toxicology

PI: Mohamad Aljofan

Co-PI: Aiman Moldasheva

A THESIS SUBMITTED

FOR THE DEGREE OF MASTER OF PHARMACOLOGY AND TOXICOLOGY

DEPARTMENT OF BIOMEDICAL

SCIENCES SCHOOL OF MEDICINE NAZARBAYEV UNIVERSITY

2024

DECLARATION

I hereby declare that the thesis is my original work, and it has been written by me in its entirety. I have duly acknowledged all the sources of information which have been used in the thesis. This thesis has also not been submitted for any degree in any university previously.

Student name: Kamila Khikhmetova

Signature: 

Date: 19.04.2024

TABLE OF CONTENTS

Abstract

Phenformin, a representative of the biguanides class, is an anti-diabetic drug that was withdrawn from the market due to its side effects profile is currently being investigated as a potential anticancer agent. Autophagy is an evolutionary conserved mechanism of lysosome-mediated catabolic breakdown of proteins, cellular compartments, and infectious agents for maintaining homeostasis. Activation of autophagy in cancer cell could potentially be one of the mechanisms of phenformin's anticancer activity. This research aimed to establish the antiproliferative activity of phenformin among different cancer cell lines and to study the effect of phenformin on expression of proteins involved in autophagy in cervical cancer cells. Cervical cancer is the fourth leading cause of cancer mortality as well as the fourth most diagnosed cancer type in females. Our findings demonstrate that phenformin decreases the proliferation of various cancer cell lines in a dose-dependent manner cells and may have an ability to increase autophagic flux in cervical cancer cells.

Keywords: phenformin, autophagy, anticancer, antiproliferative, cervical cancer

Abbreviations

4E-BP1 Eukaryotic translation initiation factor 4E binding protein 1

AMPK Adenosine monophosphate-activated protein kinase

ATG101 Autophagy-related protein 101

ATG13 Autophagy-related protein 13

BCA Bicinchoninic acid

BSA bovine serum albumin

CCA Cholangiocarcinoma

DMEM Dulbecco's Modified Eagle Medium

DMSO Dimethyl sulfoxide

DST Disseminated tumor cells

ECL Electrochemiluminescence

EGFRs Epidermal growth factor receptors

EMT Epithelial-mesenchymal transition

ER Estrogen receptor

FBS Fetal Bovine Serum

FIP00 Family interacting protein of 200kDa

HCC Hepatocellular carcinoma cells

HMGB1 High mobility group box 1

Hsc70 Heat-shock cognate protein of 70 kDa

IC50 Half-maximal inhibitory concentration

IGFRs Insulin-like growth factors

LAMP2A Lysosomal protein lysosome-associated membrane protein type 2A

mTORC1 Mammalian target of rapamycin complex 1

MTT 3-(4,5-dimethylthazolk-2-yl)-2,5-diphenyl tetrazolium bromide

NSCLC Non-small cell lung cancer

OTCs Organic cation transporters

PAS Pre-autophagosomal structure

PBS Phosphate-buffered saline

PE Phosphatidylethanolamine

PVDF Polyvinylidene fluoride

RAS Rat sarcoma virus

ROS Reactive oxygen species

RTKs Receptor tyrosine kinases

S6K1 Ribosomal protein S6 kinase beta-1

TBST Tris-buffered saline with 0.1% Tween® 20 Detergent

TCA Tricarboxylic acid cycle

ULK1 Unc-51-like kinase

List of illustrations

CHAPTER 1. INTRODUCTION

1.1 Mechanism and types of autophagy

Autophagy is an evolutionary conserved mechanism of lysosome-mediated catabolic breakdown of proteins, cellular compartments, and infectious agents for maintaining homeostasis. The process of autophagy is an important source of cellular building blocks such as amino acids, fatty acids and nucleotides for cells under basal conditions as well as those in conditions of oxygen or nutrient starvation (Mowers et al., 2017). Under basal conditions autophagy is constitutively active and serves as a mechanism protecting cells from misfolded proteins and damaged organelles (Yun & Lee, 2018). Autophagy supports the cells' constant renewal. Conditions of starvation such as low glucose and oxygen levels facilitate the process of autophagy which increases the cells' ability to survive.

Autophagy can be selective or non-selective: trafficking large parts of cytoplasm for degradation or only targeting specific structures such as damaged proteins and organelles. Autophagy is classified into three types: microautophagy, macroautophagy and chaperon-mediated autophagy (CMA). In microautophagy the cargo to be degraded is captured directly by invaginations formed in the lysosomal membrane (Parzych & Klionsky, 2014). Current knowledge of microautophagy and its role is limited due to a small number of techniques for investigating this type of autophagy. CMA assists in selective degradation of proteins with a pentapeptide motif that is recognized by heat-shock cognate protein of 70 kDa (hsc70) and it is activated during conditions of stress such as starvation. Hsc70 acts as a chaperone and is only able to recognize proteins containing specific pentapeptide motives (KFERQ motifs) at their C-terminal (Khandia et al., 2019), therefore CMA is a selective type of autophagy. Proteins then bind to a specific lysosomal protein lysosome-associated membrane protein type 2A (LAMP2A) and translocate into the lumen of the lysosome to be degraded (Khandia et al., 2019). In contrast to micro- and macroautophagy CMA does not rely on formation of vesicles for transporting the cellular components. Macroautophagy is the major and most well-studied pathway of autophagy. It will be further referred to as "autophagy".

The general mechanism of autophagy involves steps such as initiation of phagophore formation, elongation, maturation into an autophagosome, fusion with lysosome and subsequent formation of an autolysosome and degradation. Phagophore is a spherical double-membrane structure which encloses the cellular components, and it is a precursor of autophagosome (Hollenstein & Kraft, 2020). The formation of autophagic vesicles involves many autophagy related (ATG) proteins. Proteins that play a major role in the regulation of autophagy are adenosine monophosphate-activated protein kinase (AMPK), mammalian target of rapamycin complex 1 (mTORC1) and Unc-51-like kinase (ULK1) (Yun & Lee, 2018). AMPK and ULK1 increase the level of autophagy, whereas mTOR1 has been known for its inhibitory action on autophagic processes. Both AMPK and mTORC1 play key roles in cell proliferation and development, affecting a wide variety of cellular metabolic processes both in healthy and cancer cells. ULK1 complex consists of focal adhesion kinase family interacting protein of 200kDa (FIP00), autophagy-related protein 13 (Atg13) and autophagy-related protein 101 (Atg101). Under conditions where nutrients are abundant, mTORC1 blocks the activation of ULK1 complex, which is necessary for the formation of a pre-autophagosomal structure (PAS) (Li et al., 2020). Figure 1 below illustrates the process of autophagy with major stages and protein interactions responsible for

its regulation.

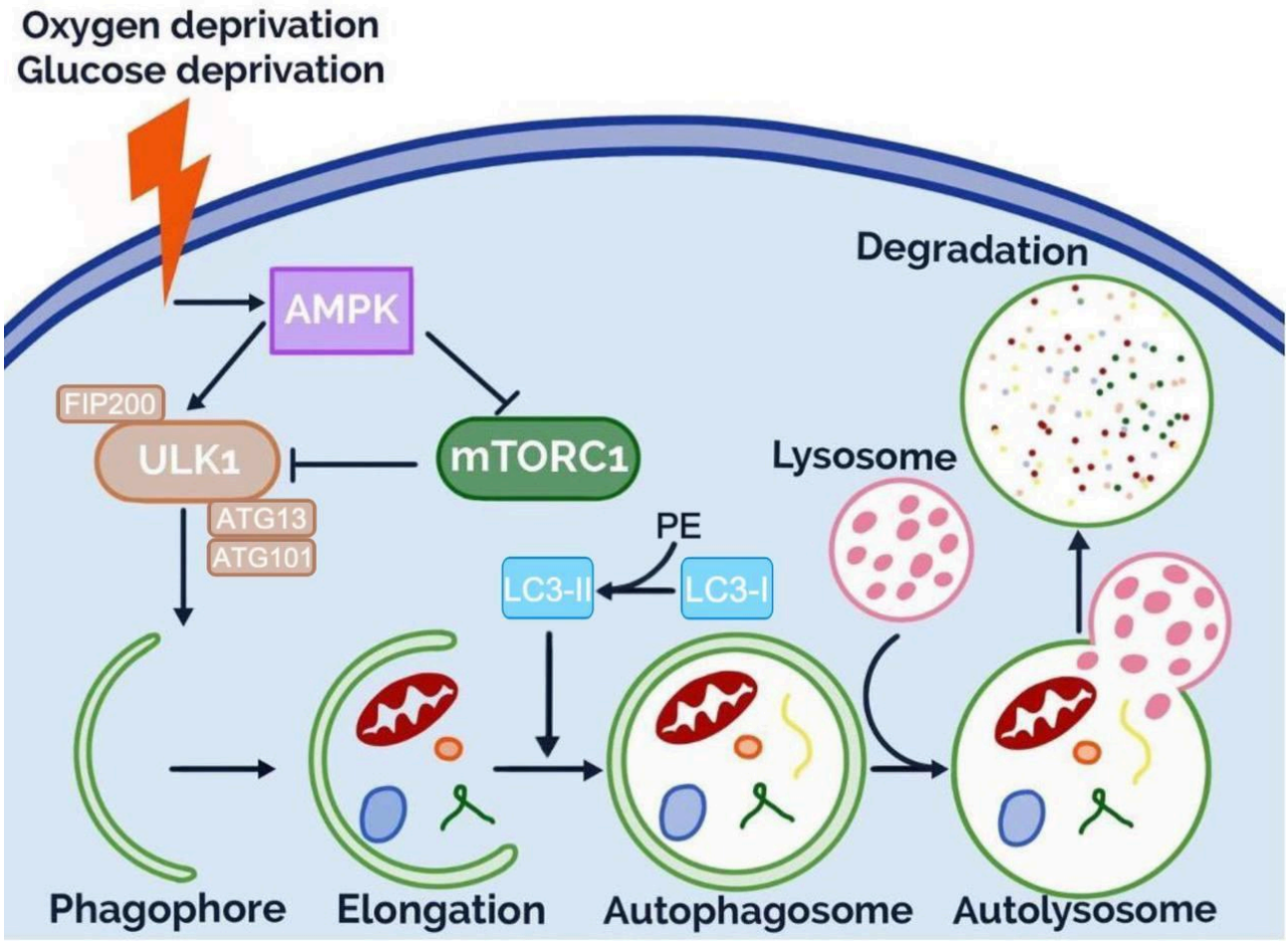

Figure 1. The process of autophagy

1.2 The role of autophagy in cancer

Interestingly, according to previous evidence, autophagy seems to have dual roles of both tumor suppression and promotion depending on the tumor type and stage (Yun & Lee, 2018; Marsh et al. 2021). Under normal conditions autophagy aids in maintenance of homeostasis by reducing reactive oxygen species (ROS), preventing damage of DNA and mitochondria (Lim et al., 2013). Accumulation of ROS inside the cell facilitates carcinogenesis and it is believed that autophagy suppresses tumor growth by selective destruction of damaged mitochondria, a process referred to as mitophagy (Ávalos et al., 2014). Additionally, autophagy was found to decrease the release of a pro-inflammatory and tumorigenic protein high mobility group box 1 (HMGB1) which results in necrosis and chronic inflammation (Khandia et al., 2019).

On the other hand, in primary tumors, loss of a protein critical for autophagy regulation the focal adhesion kinase family interacting protein of 200 kD (FIP200) which has previously been established as a component of the ULK1 complex, decreased tumor growth and metastasis (Marsh et al., 2021) which suggests a tumor promoting role of autophagy. Additionally, in the later stages of cancer development tumor cells may use autophagy as an alternative metabolic pathway to survive under conditions of starvation (Mulcahy Levy & Thorburn, 2020). Since cancer cells have high metabolic demands, it was previously theorized that they could use autophagy for nutrient supply in conditions of high demand (Ahmadi-Dehlaghi et al., 2023). Autophagy was found to promote adaptation to limited nutrients in disseminated tumor cells (DST) (Marsh et al., 2021). Cells residing in the central parts of solid tumors, where conditions are hypoxic, have high levels of autophagy activation (Yun & Lee, 2018). An abnormally increased level of autophagy has been documented in some types of rat sarcoma virus (RAS)-activated cancers, pancreatic cancer being one example (Yun & Lee, 2018). RAS are a family of proteins important for normal development and proliferation of cells, it was estimated that around 20% of all human cancers possess some form of activating mutations in RAS genes (Rajalingam et al., 2007). It was previously suggested that upregulation of autophagy may inhibit apoptosis (Tonkin-Reeves et al., 2023). Lymphoma cells treated with chloroquine, an autophagy inhibitor, were observed to have increased p53 activation and apoptosis (Amaravadi et al., 2007).

Tumor metastasis is the leading cause of cancer related deaths. It is reported that over 90% of cancer deaths are caused by tumor metastasis (Huang et al., 2018). Epithelial-mesenchymal transition (EMT) is a process during which epithelial cells undergo phenotypical changes to become mesenchymal cells with increased capacity to migrate. It was discovered that autophagy has the capacity to promote EMT in hepatocellular carcinoma cells (HCC) (Li et al, 2013). In the same study by Li et al. (2013) the invasive capacity of HCC cells was reduced upon treatment with inhibitors of autophagy or silencing of genes related to autophagy.

The controversial role of autophagy in different types and stages of cancer is one of the major factors that complicate the efforts to study the effect of this cellular process on proliferation of cancer cells.

1.3 Phenformin

Biguanides are a class of drugs used in treatment of diabetes mellitus. Metformin and phenformin are representatives of this drug class. Biguanides are derived from guanidine, a compound naturally found in plants. The chemical structures of metformin and phenformin are presented on figure 2 below.

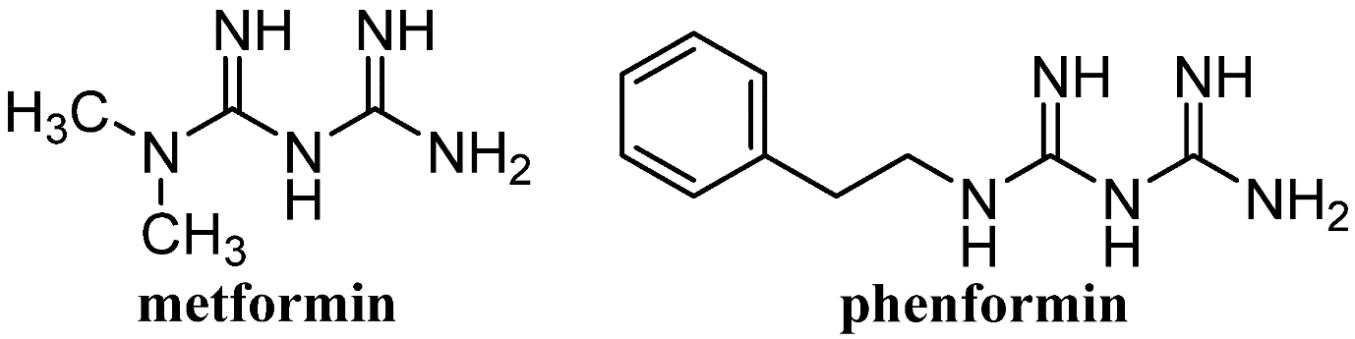

Figure 2. Chemical structures of metformin and phenformin

Metformin is currently used a first-line treatment of T2D while phenformin was removed from the market due to a higher probability of lactic acidosis. Despite that fact, phenformin is currently being investigated as a potential anticancer agent. The anticancer property of metformin has been well documented prior (Safe et al., 2018). Metformin was previously found to activate AMPK, one of the key proteins regulating autophagy. Due to its highly hydrophilic nature and possessing a positive charge at the physiological range of pH metformin requires the presence of organic cation transporters (OTCs) to enter the cytoplasm of the cells (Jackson et al., 2017; García Rubiño et al., 2019). Compared to metformin, phenformin is more lipophilic. Phenformin was reported to be 10 (Drahota et al., 2014), in some literature 30 (Janzer et al. 2014) and 50 (Garcia et al., 2019) times as potent as metformin in T2D treatment due to the fact that it directly crosses the cellular membrane to exert its effect and does not need assistance of OCTs. For the same reason, it is theorized that phenformin may serve as a more effective tool in cancer treatment compared to metformin. A study by Appleyard et al. (2012) confirmed the higher potency of phenformin to treat estrogen receptor (ER) positive and negative breast cancer xenografts *in vivo* in mice.

Currently, there is a dearth of studies on potential anticancer effects of phenformin and its precise mechanism of action. Potential therapeutic repurposing of phenformin as an anticancer agent would benefit patients with cancer at large, but especially those with tumors which do not respond to currently available treatment methods such as chemotherapy.

1.4 Proposed mechanisms of antiproliferative activity of phenformin

Based on previous studies, several potential mechanisms for the activity of phenformin in inhibiting cancer cell growth have been proposed. These mechanisms include apoptosis (Miskimins et al., 2014) and autophagy (Hu et al., 2018), suppression of loss of contact inhibition (Janzer et al., 2014), inhibition of mitochondrial complex I (Garcia et al., 2019), inhibition of epithelial-mesenchymal transition (Garcia et al., 2019) and G1 cell cycle arrest (Geoghegan et al. 2017).

Apoptosis, also known as programmed cell death, might be one of the mechanisms by which phenformin destroys cancer cells. Cholangiocarcinoma (CCA) is a cancer of bile ducts. It was found that a statistically significant proportion of CCA cells treated with 2 mM phenformin for 24 hours underwent apoptosis (Hu et al., 2018). Cleaved PARP (cPARP) is an indicator of caspase-dependent apoptosis, and its increase was detected in phenformin treated colon cancer cells (Miskimins et al., 2014).

In a study on morphologic transformation of the immortalized breast epithelial cell line Janzer et al. (2014) found that phenformin resulted in a comparable effect of suppressing the loss of contact inhibition even if the concentration of phenformin used was 30 times lower than that of metformin. Loss of contact inhibition results in uncontrolled cell growth and may increase the likelihood of tumor metastasis (Pavel et al., 2018). Therefore, suppression of the loss of contact inhibition can have the potential to slow down or stop metastasis of cancer cells.

Like metformin, phenformin was also found to inhibit mitochondrial complex 1. Inhibition of mitochondrial complex I and subsequent activation of AMPK leads to an increase in AMP/ATP ratio and accumulation of ROS (Garcia et al., 2019). Overproduction of ROS leads to cell death.

Tricarboxylic acid cycle (TCA), also referred to as the Krebs cycle and citric acid cycle, is one of the most important metabolic pathways supplying biomolecules necessary for cell survival as well as energy via indirect ATP generation. Both metformin and phenformin were found to decrease the amount of TCA intermediates in cells undergoing tamoxifen-induced neoplastic transformation (Janzer et al., 2014).

Phenformin was also proposed to inhibit EMT by blocking metabolic pathways associated with activation of receptor tyrosine kinases (RTKs) such as epidermal growth factor receptors

(EGFRs) and insulin-like growth factors (IGFRs) (Garcia et al., 2019). Administration of phenformin was found to decrease markers of EMT in ErbB2-overexperssing human breast cancer cell line (Guo et al., 2017). Additionally, both metformin and phenformin resulted in a decrease in the expression levels of mesenchymal markers such as N-cadherin, vimentin, Snail, Twist, Slug and Zeb1 in rectal cancer cells (Park et al, 2019).

Geoghegan et al. (2017) found that administration of phenformin resulted in a reduction of cell viability in the neuroblastoma SH-SY5Y cell line. Additionally, they discovered that there was an increase in the G1 population among phenformin treated cells and suggested that phenformin may have the capacity to induce G1 cell cycle arrest. The inhibitory effects of phenformin on cell proliferation were also confirmed in a variety of ovarian cancer cell lines such as SKOV3, Hey and IGROV-1 (Jackson et al., 2017).

1.5 Relationship between phenformin and autophagy

Inhibition or activation of autophagy in cancer cell could potentially be one of the mechanisms of phenformin's anticancer activity. AMPK is one of the key regulators of autophagy along with mTOR1 and ULK1, since phenformin activates AMPK, it may have an indirect effect of inducing autophagy in cancer cells. Metformin was previously found to slow down the rate of tumor growth in cancer of cervix and melanoma by inducing autophagy via activation of AMPK (Lim et al., 2021). Increased phosphorylation of AMPK and decreased phosphorylation of S6 in three ovarian cancer cell lines showed that phenformin activates AMPK and inhibits mTOR (Jackson et al., 2017). In a study by Hu et al. (2018) CCA cells treated with 2 mM phenformin were observed to have a significantly higher level of mRNA of genes associated with autophagy such as autophagy 5, autophagy 7 (ATG5 & ATG7) and Beclin-1 resulting in an increase in autophagy.

Some studies show that despite its AMPK-activating effects phenformin may not lead to induction of autophagy and instead could inhibit autophagy induced by other factors such as exogenous stress and drugs. Thomas et al. (2018) found that phenformin inhibited autophagy induced by mTOR inhibitors and did not induce autophagy at varying doses (ranging from 0.02 to 5 mM).

Current evidence highlights the uncertain effects of phenformin on autophagy. As mentioned in the previous section, this could be related to a controversial role of autophagy in both suppression

and progression of tumors. Since activation of AMPK by phenformin was not found to induce autophagy, phenformin may have an indirect effect on autophagy which could be mediated by a pathway other than AMPK.

1.6 Hypothesis and objectives

In this study, we hypothesize that phenformin may mediate its antiproliferative effects via promotion of autophagy. Since autophagy is known to have dual effects of both tumor suppression and progression and the reported effects of phenformin on autophagy are also uncertain, there is a necessity to firstly determine a cancer cell line which will be most susceptible to phenformin. Secondly, we aim to study the impact of phenformin on autophagy as a mechanism of its antiproliferative potential by monitoring changes in expression of autophagy related proteins such as p62 and LC3.

CHAPTER 2: MATERIALS AND METHODS

2.1 Cell culture

To study phenformin's potential anticancer activity in the first part of the experiment 7 different human cancer cell lines were obtained and seeded along with 1 non-tumorigenic epithelial

cell line as a control. Table 1 below indicates the names and classes to which the studied cell lines belong.

Table 1. Cell lines used in the study

A375	Malignant melanoma
HS-578	Breast cancer
HUH7	Hepatocellular carcinoma
Capan-2	Pancreatic cancer
MCF-7	Breast cancer
Dotc4510	Cervical cancer
MCF-10	Human breast epithelium

Cells were cultured in Dulbecco's Modified Eagle Medium (DMEM) containing glucose in concentration of 4.5g/mL and supplemented with 10% Fetal Bovine Serum (FBS) and 5% of penicillin and streptomycin (Gibco). Initially the cells were cultured in T25 tissue culture flasks and then passaged into tissue culture containers appropriate for the experiment of interest (6-well plates, 96-well plates, T75 flasks). Tissue culture flasks and well plates containing the cells were incubated at 37°C and 5% CO2 (Binder CO2 incubator, Model CB-S 170).

Growth medium change protocol: The growth medium was changed every 1-2 days. The old medium was carefully aspirated, and the flask was rinsed with 1 x phosphate-buffered saline (PBS) to further remove any remaining cellular debris and traces of old media prior to addition of the new media. The volumes of PBS and new media were adjusted according to the size of the flask.

Passaging cells: The steps of discarding old media and rinsing with 1x PBS were performed identically to those in the growth medium change protocol when the cells reached at least 70% confluency. The PBS was then aspirated, and an appropriate volume of trypsin was added (1 ml for T25 flask, 2ml for T75 flask). The cells were incubated at 37 in the CO incubator for 3-5 minutes until sufficient detachment has occurred. An appropriate volume of medium was added to stop the trypsinization process (4 ml for T25 and 8 ml for T75 flasks). The medium with cells was collected,

placed into a 15 ml Falcon tube and centrifuged at 100 rpm for 5 minutes. The supernatant was discarded and the pellet was resuspended in 1 ml of media. If necessary, the cell count was performed at this stage. If the cell count was not necessary 500 µl (or less, depending on the cells' growth rate and confluency at the time of passaging) of the cell suspension were transferred into a new T25 or T75 flask containing fresh media and incubated at 37°C and 5% CO2.

Cell counting protocol: 20 µl of cell suspension were mixed with 80 µl of media and 100 µl of Trypan Blue dye. A small amount of the resulting solution was pipetted onto the Neubauer Improved hemocytometer with counting grid. The number of cells on the 4 squares located near the edges of the grid was counted and the final concentration of the cell suspension was calculated according to the following formula:

$$\frac{Total\ number\ of\ cells\ in\ 4\ squares}{4}\ x\ 10\ x\ 10^4 = Final\ cell\ concentration\ (cells/ml)$$

Where 4 is the number of squares and 10 is the dilution factor (DF).

2.2 Drug preparation

A stock solution of 100 mM phenformin was prepared by dissolving 0.13g of phenformin hydrochloride in 5 ml of double distilled water. Prior to application the stock solution was diluted in media to yield a highest concentration of 5 mM phenformin for the MTT assay, where its serial dilution was performed. The concentration range used in this study was based on concentrations of phenformin used in previous studies found upon literature search. In three ovarian cancer cell lines phenformin showed effectiveness in decreasing cellular proliferation at a range of 0.01-2.5 mM (Jackson et al., 2017). The same stock solution was also used for Western blot detection of autophagy related proteins, however the concentration of phenformin was diluted to the half-maximal inhibitory concentration (IC50) value of a given cell line. The IC50 of phenformin for the most sensitive cell line, DoTc-4510 was determined to be 0.14 mM. To achieve a concentration of 0.14 mM in 2 ml of media for a single well of a 6-well plate, 2.8 µl of 100 mM phenfomin were diluted in 1997 µl of media. Galangin, a known autophagy inducer, was used as a positive control. To prepare a 5 mM stock solution 1.35 mg of galangin were dissolved in 1ml of dimethyl sulfoxide (DMSO). The stock solution was then diluted with culture medium to yield a 50 µM final solution of galangin which was used to treat the cells for the Western blot procedure.

2.3 Cell viability assay

To assess phenformin induced changes in cell viability 3-(4,5-dimethylthazolk-2-yl)-2,5-diphenyl tetrazolium bromide (MTT) assay was performed. Reagents from the Cell Proliferation Kit I (MTT), Sigma Aldrich were used. Cells were seeded in a 96-well plate at density of 3000 cells per well in triplicates. The total volume of cells and media in each well equaled 100 µl. The next day cells were treated with phenformin at varying concentrations ranging from 5 mM to 0,0068 mM which were obtained using serial dilution. To achieve the highest 5 mM concentration 8 µl of 100 mM stock solution was added. A schematic representation of the placement of cells and different drug concentrations on the 96-well plates is shown on figure 3 below.

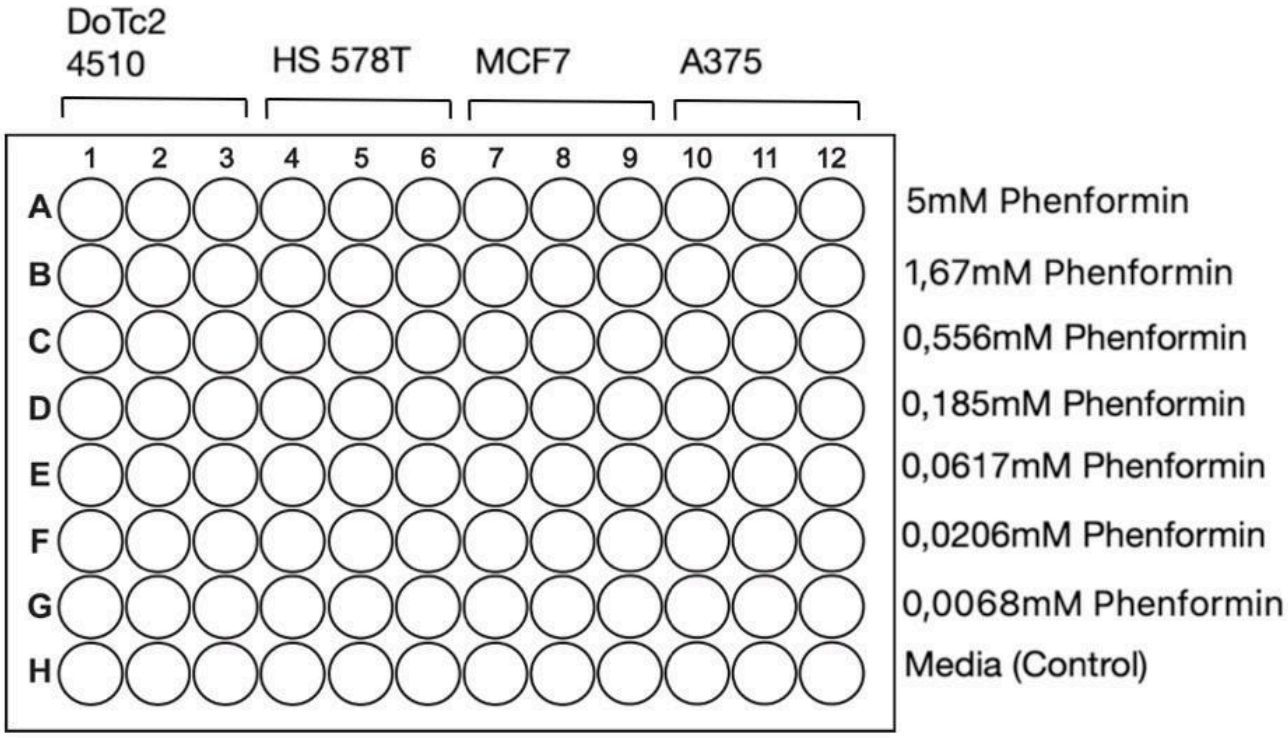

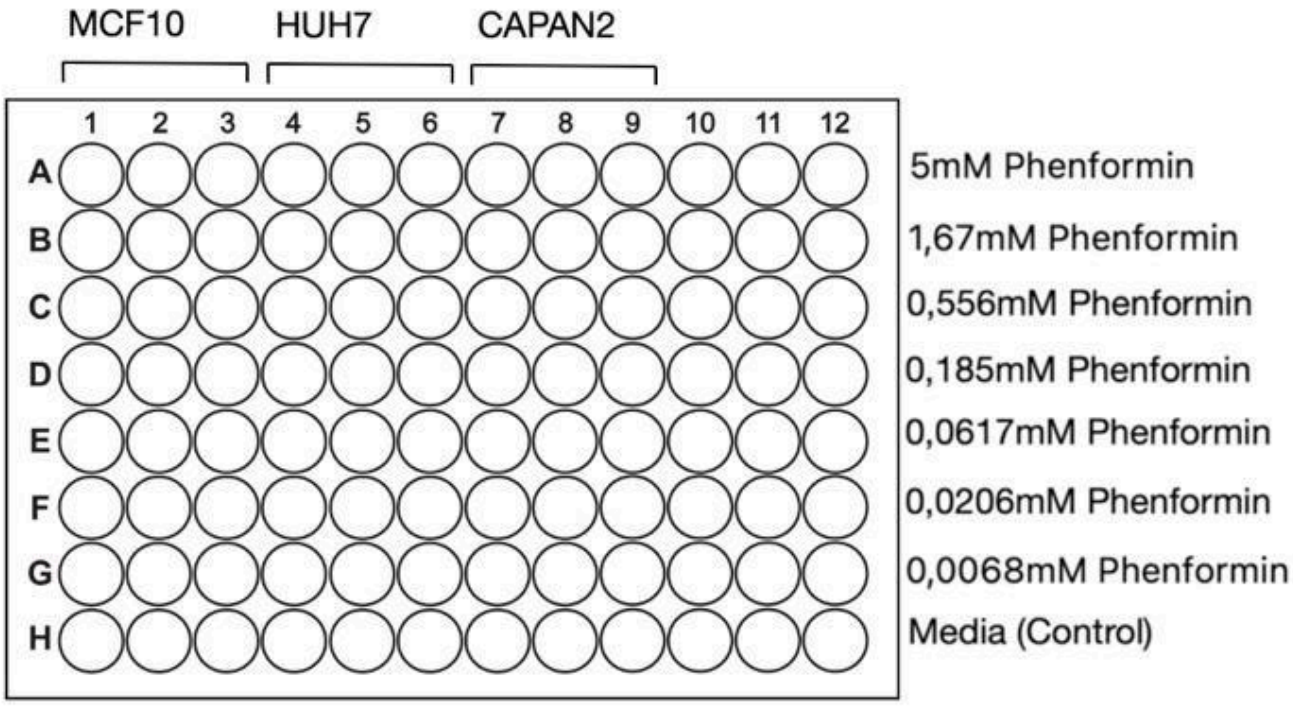

Figure 3. 96-well plate placement schemes

48 hours after drug treatment 10 µl of MTT labelling reagent was added to each well and the plates were incubated at 37°C and 5% CO2 for 4 hours. After 4 hours of incubation 100 µl of solubilization buffer was added to each well and incubated overnight. The next day the 96-well plate was evaluated using an iMark™ Microplate Absorbance Reader (Bio-Rad) at wavelength of 595 nm and quantitatively presented using the Microplate Manager Software (Bio-Rad). To perform reading of the plate it was wrapped on aluminum foil during transfer from the incubator to the reader to avoid inaccuracies due to the light sensitive nature of the assay. The percentage of cell viability was calculated by taking the value of absorbance of cells treated with phenformin at different concentrations and dividing it by the absorbance value of untreated controls. The data was analyzed and plotted using the GraphPad Prism software. From this data the half-maximal inhibitory concentration (IC50) of phenformin for each cell line was determined.

2.4 Protein extraction and quantification

Protein extraction: The cells were seeded in a 6-well plate at a density of $3x10^5$ cells per well. The total volume of cells and media for each well was 2 ml. The next day after seeding the cells were treated with phenformin (0.14 mM), galangin (50 µM) and a combination of phenformin and galangin. 48 hours after drug treatment the medium containing the drug was carefully removed

and the cells were washed with 2ml of ice cold 1xPBS 2 times. The microplate itself was kept on the ice as well. To disrupt the cells and allow for protein extraction to take place 150 μM of cold radioimmunoprecipitation assay (RIPA) buffer was added to each of the wells. Cells were scraped from the bottom of the wells and transferred into pre-labelled 1.5 ml Eppendorf tubes. Tubes with samples were constantly agitated for 30 minutes at 4°C. To complete cell lysis, sonication of samples for 15 seconds was performed 3 times. The tubes were then centrifuged at 16000 x g for 20 minutes at 4°C. The supernatant was transferred to new pre-labelled 1.5 ml Eppendorf tubes. After 10 μl of the samples were pipetted into PCR tubes for protein quantification, the remaining volume of samples were placed into a -20°C freezer for storage prior to the Western blot.

Protein quantification: For quantification a bicinchoninic acid (BCA) assay kit from Thermo Fisher was used. Standards were prepared according to manufacturer's protocol by diluting albumin in RIPA buffer (concentration was ranging from 2mg/ml to 0,025mg/ml). RIPA buffer without albumin was used as a blank. Due to limited sample size, 2 μl of each sample was pipetted and diluted in 8 μl of RIPA buffer in triplicates into a 96-well. The standards were pipetted in volume of 10 μl as per protocol. The working reagent solution was prepared by mixing 50 parts of Reagent A with 1 part of Reagent B provided in the kit and 200 μl of working reagent was added to each well. The plate was covered and incubated at 37°C and 5% CO2 for 30 minutes. The absorbance was measured at 575 nm. A standard curve was prepared by plotting the average of blank-adjusted BCA standard absorbance values vs their known concentration. The equation of the standard curve was used to calculate protein concentration for all unknown samples.

2.5 Western blot

During western blotting the expression of autophagy related proteins mTOR (286kDa), p62 (60-62kDa) and LC3 (17kDa) was measured. Due to a large difference in molecular weights the proteins were visualized on gels of different percentages: a 7% gel was used for mTOR and p62 and a 15% gel was used for LC3.

Sample preparation: Since protein content of samples was different, the volume had to be adjusted to yield an equal amount of 20 μg of protein per well. The samples and 2X Laemmli buffer with mercaptoethanol were mixed in 1:1 ratio in an Eppendorf tube and put in an Eppendorf ThermoMixer Shaker heated to 95°C for 5 minutes. Before loading sample containing tubes were also centrifuged at 16,000 x g in a microcentrifuge for 1 minute.

Protein separation and transferring: For gel preparation and running the Mini-PROTEAN Tetra Cell (Bio-Rad) gel electrophoresis system was used. Before protein loading and transferring fresh 1X Running and 1X Transferring buffers were prepared. After loading the sample, the gel was run at 50V for 5 min. The voltage was increased to 125V for 1,5 hours. The proteins were transferred overnight at 30V in the cold room using a wet/tank blotting system. For transferring a polyvinylidene fluoride (PVDF) membrane activated in methanol was used. The transfer sandwich was assembled using 2 foam pads and 2 filter papers, between which the membrane and gel were placed and gently pressed together to avoid formation of air bubbles that might have interfered with transfer.

Antibody incubation: When the overnight transfer was finished the membrane was taken out and placed in a solution of 1% bovine serum albumin (BSA) in Tris-buffered saline with 0.1% Tween® 20 Detergent (TBST) for blocking for 1 hour at room temperature. After that, the membrane was rinsed 3 times with TBST for 5 minutes. Primary antibody incubation was performed at room temperature for 1 hour on a shaker to achieve even coverage of the membrane. To remove traces of unbound primary antibody the membrane was rinsed 3 times with TBST for 5 minutes. The steps involving incubation of the membrane with HRP-conjugated secondary antibody and rinsing with TBST were identical to those described for the primary antibody. Since primary antibodies that were used in this experiment were obtained from different hosts, the secondary HRP-conjugated antibodies were prepared for both rabbit and mouse hosts and applied according to the species of origin. Table 3 contains information on primary and secondary antibodies used in this study along with their origin and dilution ratio.

Table 3. List of antibodies

Antibody	Host species	Dilution ratio	Solvent
Primary anti-P62	Mouse	1:5000	1% BSA in TBST
Primary anti-LC3	Rabbit	1:2000	1% BSA in TBST
Primary anti-mTOR	Rabbit	1:500	1% BSA in TBST
Primary anti-α-tubulin	Mouse	1:20000	1% BSA in TBST

Primary anti-GAPDH	Rabbit	1:5000	1% BSA in TBST
Secondary anti-rabbit	Goat	1:5000	1% BSA in TBST
Secondary anti-mouse	Goat	1:5000	1% BSA in TBST

Imaging and data analysis: Prior to imaging the membranes were treated with a chemiluminescent substrate Clarity Western Electrochemiluminescence (ECL), Bio-Rad. The substrate was prepared by mixing equal volumes of Clarity Western peroxide reagent and Clarity Western luminol/enhancer reagent. Imaging of the blot was performed with the ChemiDoc MP Imaging System (Bio-Rad). Digital images of the bands present on the membrane were obtained using Image Lab Software (Bio-Rad). Quantification of bands based on their intensity was performed in ImageJ software and graphically presented using GraphPad Prism.

CHAPTER 3: Results

3.1 Phenformin induced changes in cell viability

Based on data obtained from three replications of the MTT assay for all studied cell lines, percentage viability was calculated and plotted against base 10 logarithm of phenformin concentrations in GraphPad Prism software. Half maximal inhibitory concentration (IC50) was calculated for all 7 cell lines used in this study.

One of the important findings was the fact that almost all of the studied cell lines showed a dose-dependent decrease in cell viability upon treatment with different concentrations of phenformin after 48 hours. One cell line, more specifically capan-2 pancreatic cancer, had a markedly large increase in cellular proliferation at three lowest concentrations of phenformin. This finding was unexpected and was also confirmed with another biguanide metformin applied at the same concentrations (Figure 4s), indicating a need for further research on potential pro-proliferative effect of biguanides on pancreatic cancer cells.

It was determined that DoTc-4510 cervical carcinoma cell line was the most sensitive to antiproliferative effects of phenformin. Its IC50 value was determined to be 0.1436 mM and it was the lowest among all studied cell lines, meaning that a smaller concentration of phenformin is necessary to achieve a 50% viability reduction in DoTc-4510 cells compared to other cells lines. Figures 4-10 below illustrate individual cell viability curves with standard deviation and their IC50 values calculated in GraphPad Prism along with description of main points.

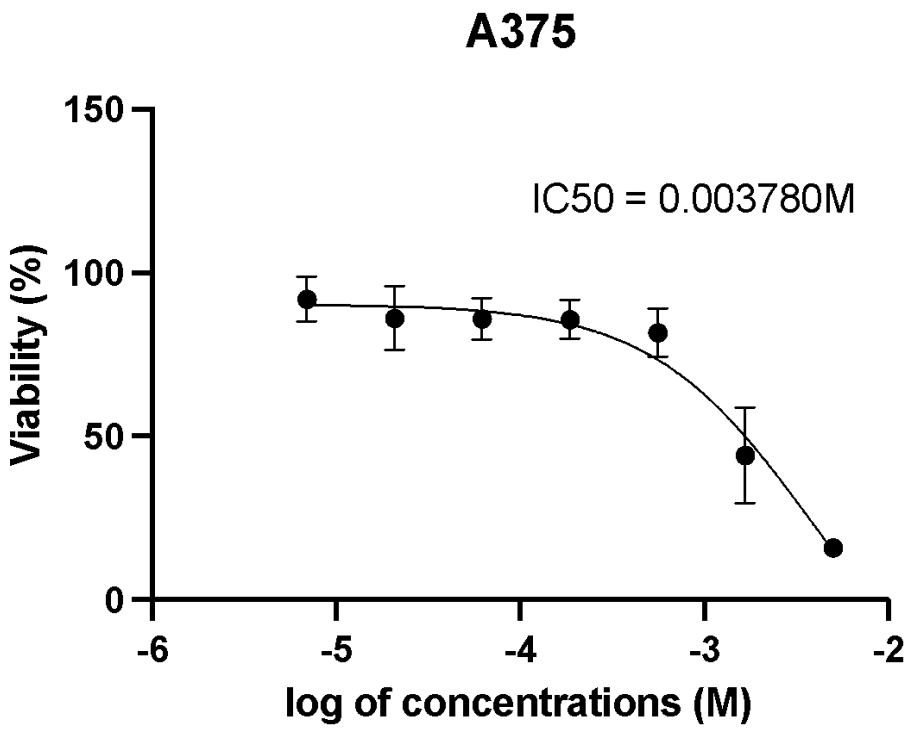

Figure 4. Cell viability curve of A375

The viability of A375 cells remains fairly constant at five lowest concentrations of phenformin and decreases dramatically at two highest concentrations of 1.66 mM and 5 mM. 48 hours after treatment with 5 mM phenformin the percentage viability of malignant melanoma cells was equal to 15% on average among all three replates of the MTT assay. IC50 was found to equal 0.003780 M or 3.78 mM. Despite such a dramatic decrease at higher concentrations, based on the IC50 values A375 cell line was among the least sensitive to antiproliferative effects of phenformin, along with HS 578T and HUH7.

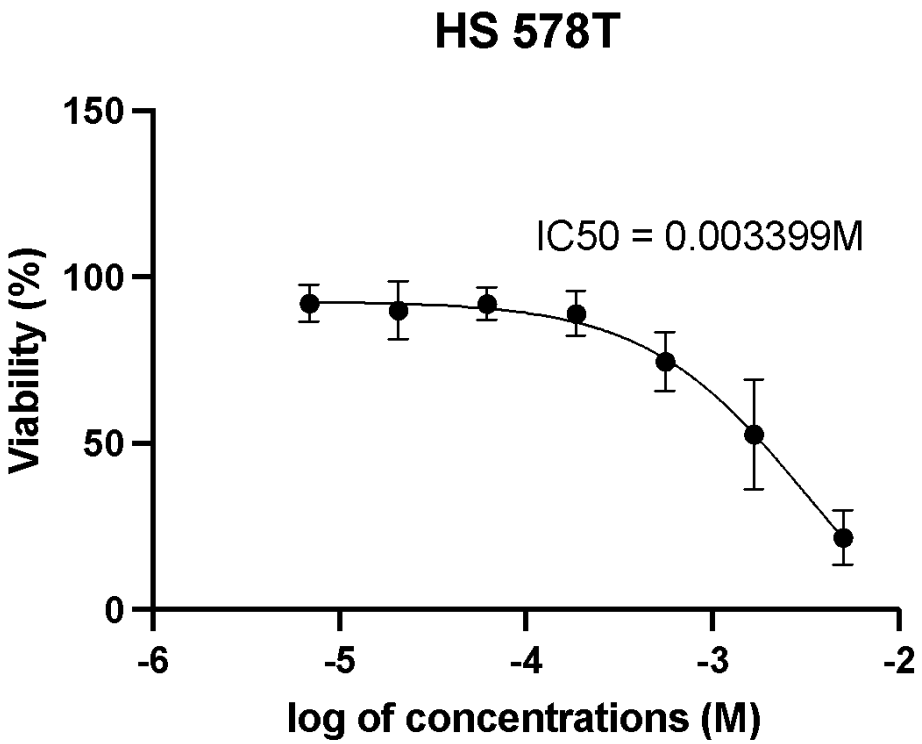

Figure 5. Cell viability curve of HS 578T

The viability of HS 578T cells remains fairly constant at four lowest concentrations of phenformin and starts to decease at around 0.556 mM. IC_{50} was calculated to be 0.003399M or 3.4 mM.

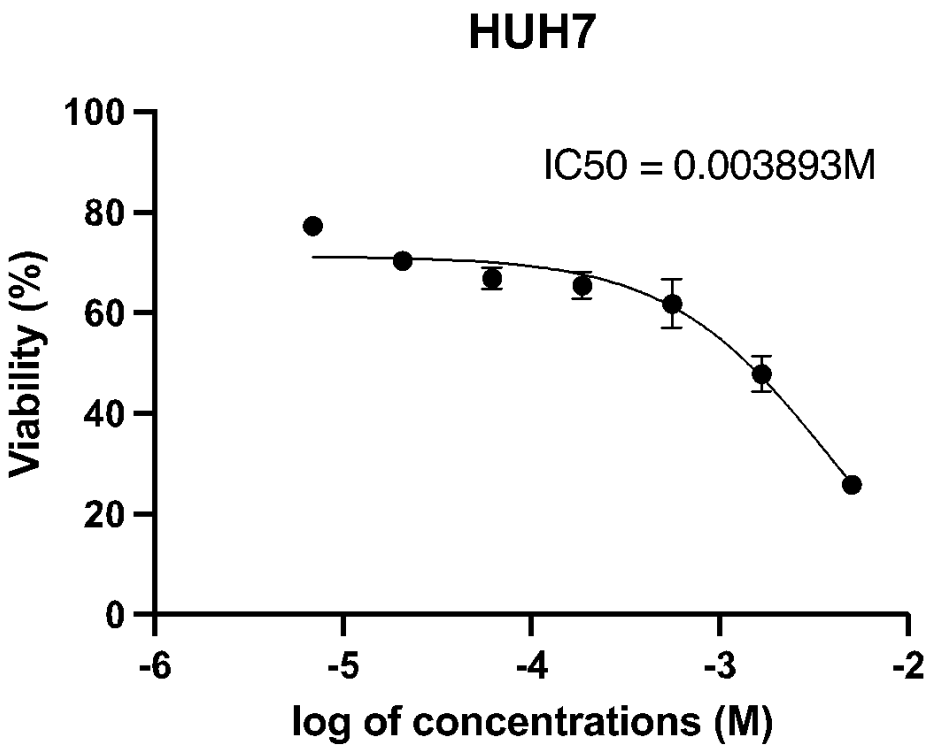

Figure 6. Cell viability curve of HUH7

For HUH7 hepatocellular carcinoma cell line the IC50 was determined to be 0.003893M or 3.9mM.

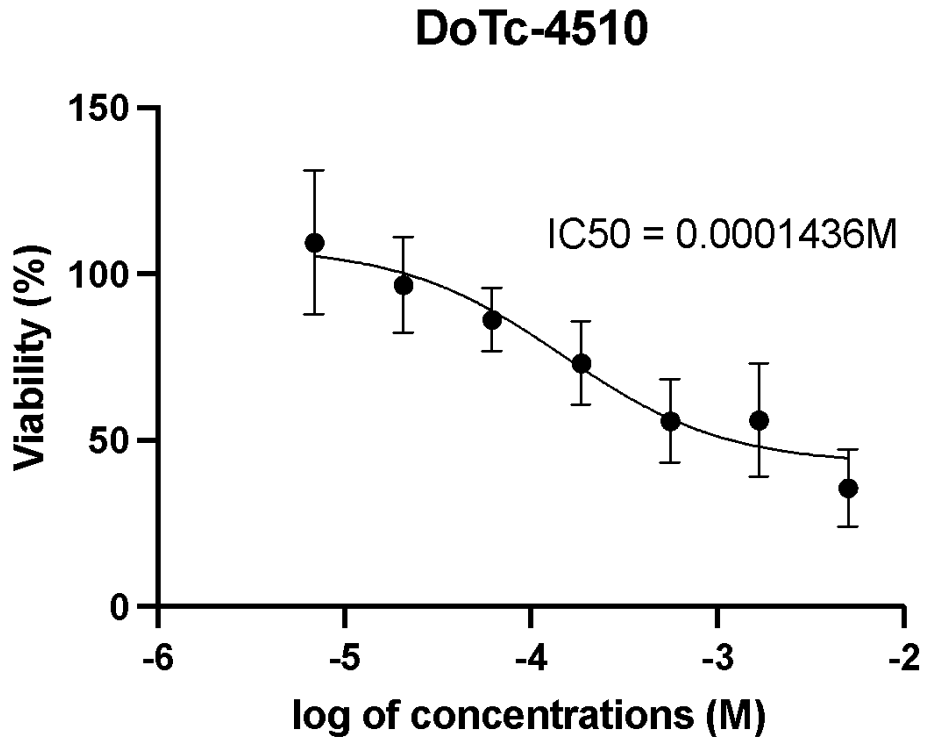

Figure 7. Cell viability curve of DoTc-4510

Viability of DoTc-4510 cells was observed to decrease at almost all concentrations. At lowest concentration of phenformin (0.0068 mM) the viability of cervical cancer cells was slightly above that observed in untreated control. At highest concentration of phenformin (5 mM) the average percent viability value was around 35%. The DoTc-4510 cell line had the smallest IC50 value of 0.0001436 M or 0.1436 mM and was considered the most sensitive in terms of its response to phenformin.

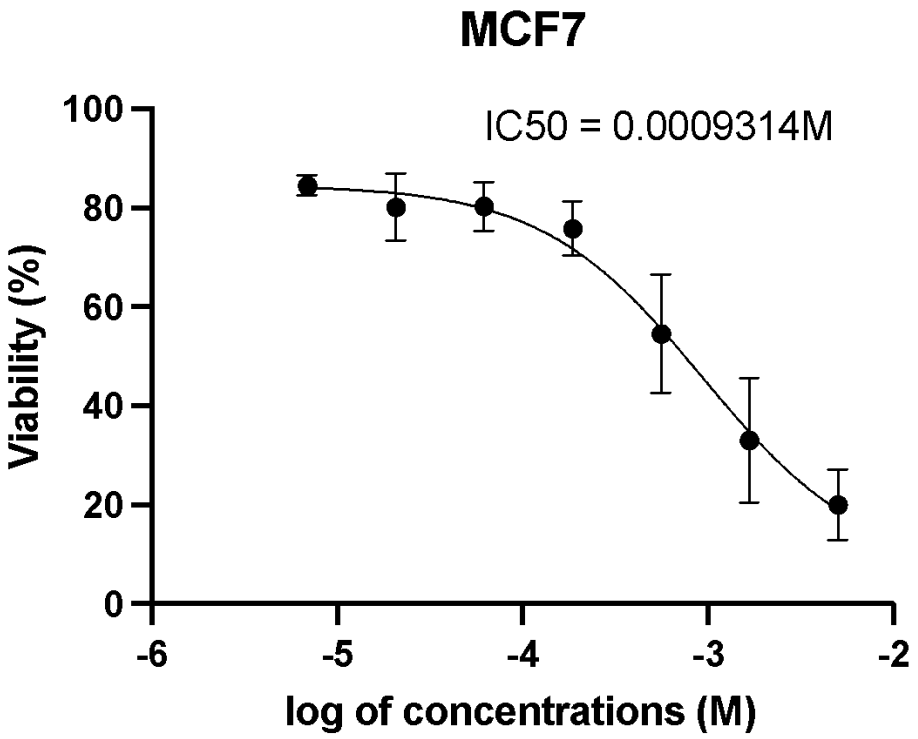

Figure 8. Cell viability curve of MCF7

The maximum viability achieved by MCF7 breast cancer cells at lowest concentration of phenformin at 0.0068 mM was 84%. The viability of MCF7 cells was also found to decrease below 40% at two highest concentrations of phenformin (5 mM and 1.66 mM). The IC50 of MCF7 cell line for phenformin treatment was found to equal 0.0009314 M or 0.9314 mM. Notably, in a previous study by Liu et al. (2015), using the Cell Counting Kit-8 (CCK-8) assay, the IC50 of the MCF7 cell line was determined to be 1.184 mM, this value is close to the one that we found despite using a different colorimetric assay.

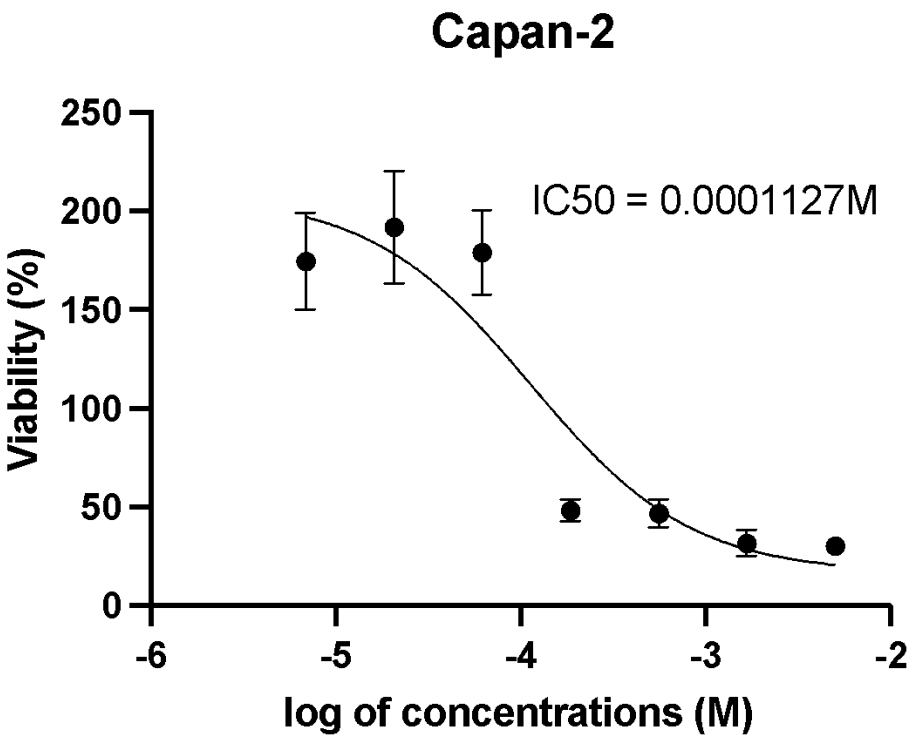

Figure 9. Cell viability curve of Capan-2

Surprisingly, three lowest concentrations of phenformin (0.0068 mM, 0.0206 mM and 0.0617mM) were found to have a pro-proliferative effect on Capan-2 pancreatic cancer cells, as the viability of cells treated with these concentrations were above 100% observed in untreated controls. At four highest concentrations cell viability decreased below 50%. The IC50 was found to equal 0.0001127 M or 0.1127 mM which is lower than that observed in DoTc-4510, however Capan-2 were not considered the most sensitive cell line due to the fact that some concentrations appeared to be pro-proliferative in all three replicates of MTT assay.

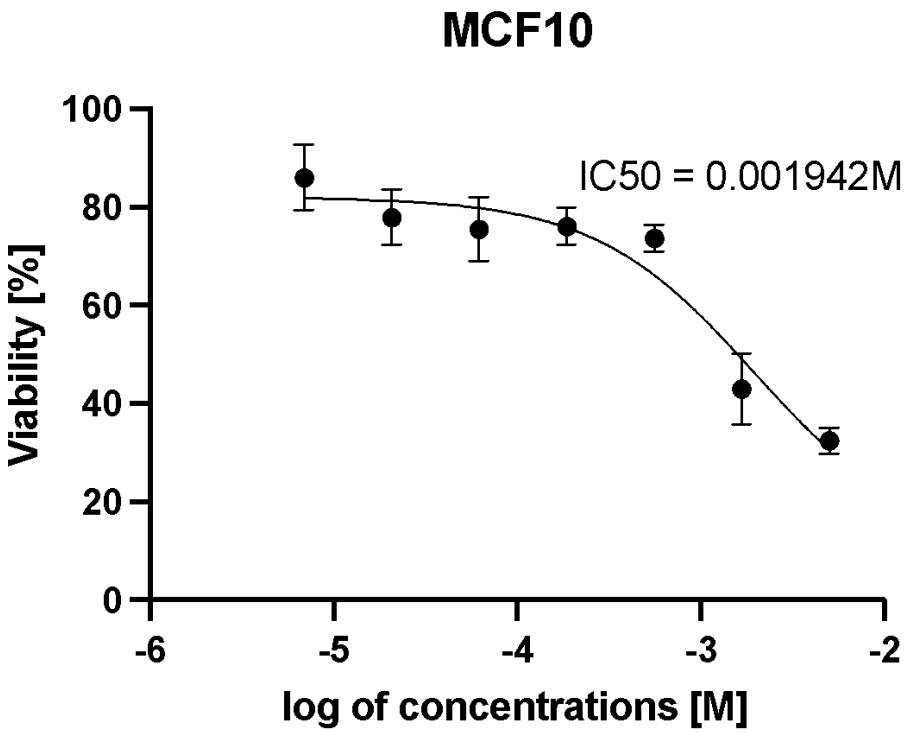

Figure 10. Cell viability curve of MCF10

IC50 of MCF10 breast epithelial cells was calculated to be 0.001942 M or 1.942 mM. In this part of the study, MCF10 non-cancerous healthy epithelial cells were used as a control for cytotoxic effects of phenformin. It was shown that at higher concentrations of 5 mM and 1.66 mM the viability of MCF10 cells decreases below 50%, indicating that cytotoxic effects of phenformin may not be limited to tumor cells. Notably, it was found that two breast cancer cell lines used for this study, MCF7 and HS 578T respond differently to phenformin based on a difference in their IC50 values of 1.942 mM and 3.4 mM, respectively.

3.2 Expression of autophagy related proteins from the western blot

The IC50 calculated in the first part of the experiment was then used for treatment of DoTc-4510 cells for the western blot. Galangin, a naturally derived flavonoid and a known autophagy inducer which was also previously suggested to have anticancer activity (Wang & Tang, 2017), was used as a positive control for autophagy. It was applied at a concentration of 50 μM to cells both separately and in combination with phenformin at IC50. If antiproliferative effect of phenformin was mediated via induction autophagy, we expected to see a synergistic effect of increasing pro-autophagic protein expression when phenformin and galangin were in combination, and vice versa if phenformin inhibited autophagy.

The proteins of interest related to autophagy which were detected during the western blotting were mammalian target of rapamycin (mTOR), sequestosome 1 (p62/SQSTM1) and microtubule‐associated protein light chain 3 (LC3) with molecular weights (MW) of 289, 62 and 17, respectively. Loading controls were used to normalize the proteins levels.

Different loading controls, GAPDH (MW 36) and α-tubulin (MW 50), were used for each blot to ensure that there is a significant difference in mass between our proteins of interest and loading controls to avoid potential band overlap or other signal disturbances. Since α-tubulin (MW50) and p62 (MW 60-62) are close in molecular weight it was decided to use GAPDH as a loading control for the blot treated with antibodies against mTOR and p62. α-tubulin was used in the blot treated with antibodies against LC3 due to the fact that α-tubulin has a larger difference in molecular weight with LC3 than does GAPDH.

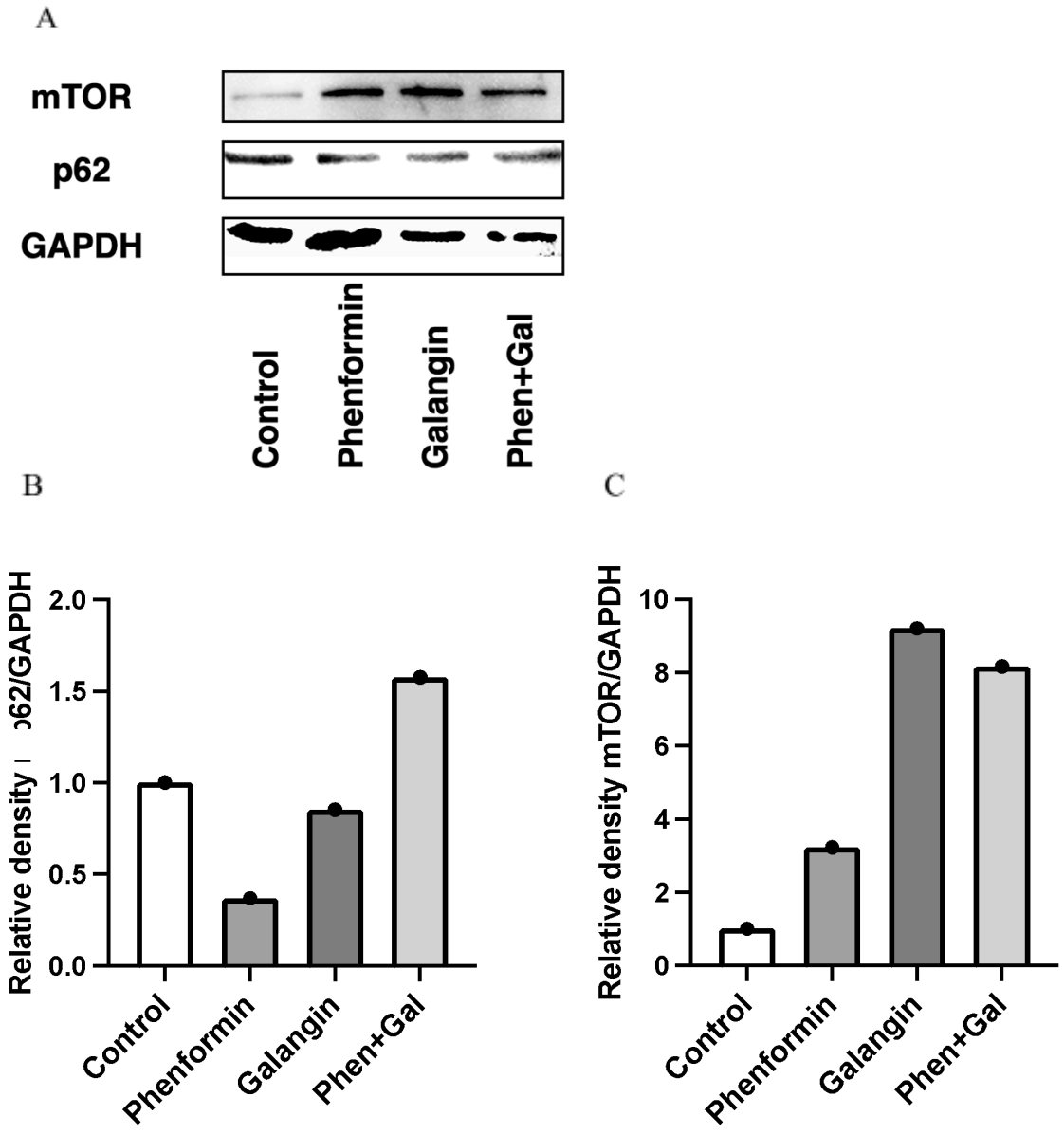

Figure 11. Western blot quantification of mTOR and p62 proteins levels (N = 1). (A) Protein expression levels of mTOR, p62 and GAPDH following treatment of DoTc-4510 cells for 48 hours with 0.144mM phenformin. (B) Graph showing the relative mTOR protein level adjusted with GAPDH. (C) Graph showing the relative p62 protein level adjusted with GAPDH.

From the bands obtained for the loading control GAPDH it is evident that despite calculating the protein amount from the BCA assay the samples were loaded unevenly. To adjust for that, the densities of mTOR and p62 proteins were divided by the relative densities of GAPDH.

The relative density of mTOR was markedly increased in all drug treated samples compared to control. In galangin only treated sample the density of mTOR increased more than 9 times, and in cells treated with a combination of phenformin and galangin it was increased 8 times.

The relative density of p62 is decreased more than two-fold in phenformin treated cells, a small decrease in galangin treatment group is also apparent. P62 expression was increased 1.5 times in cells treated with a combination of phenformin and galangin.

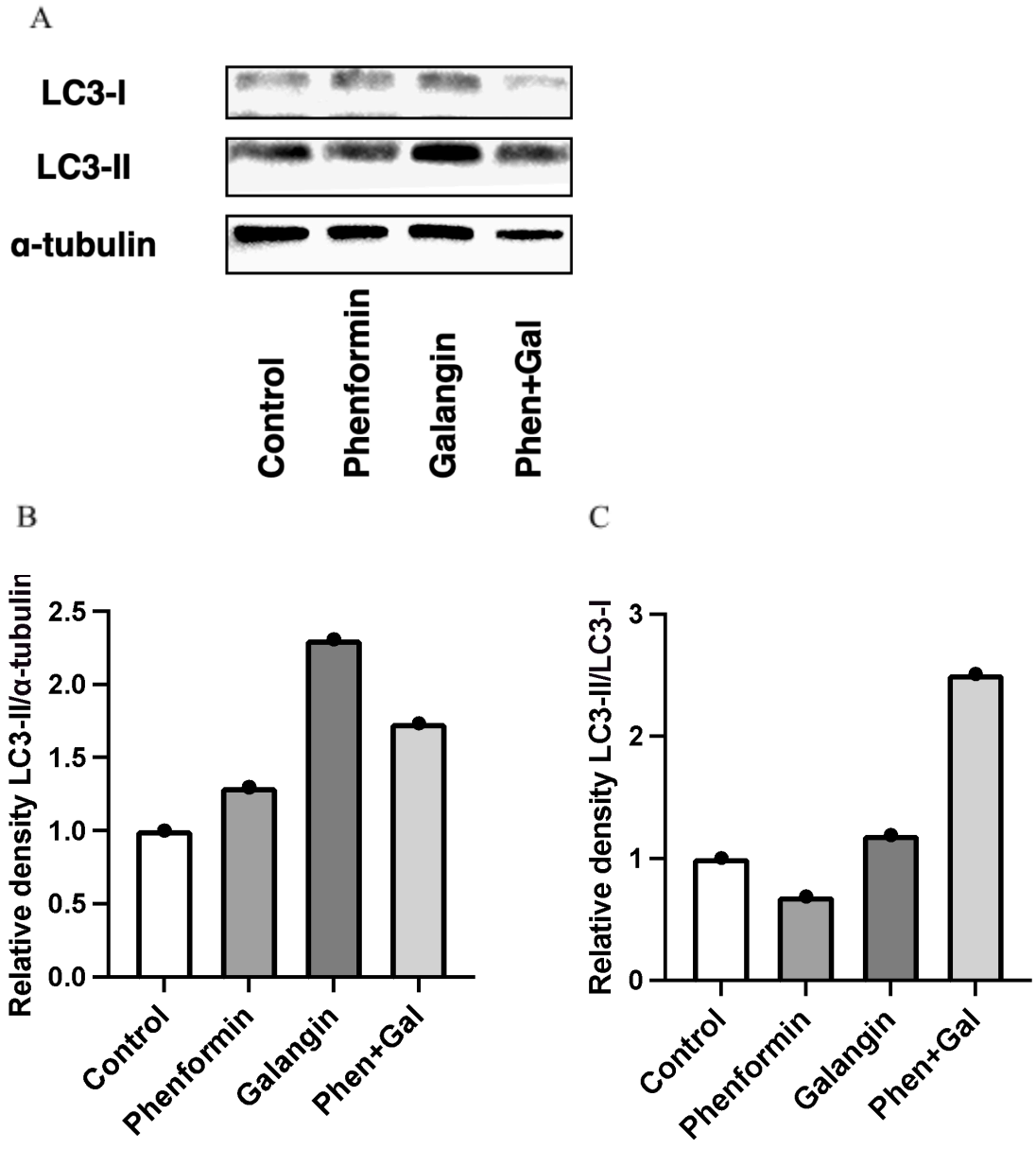

Figure 12. Western blot quantification of LC3-I and LC3-II proteins levels (N = 1). (A) Protein expression levels of LC3-I, LC3-II and α-tubulin following treatment of DoTc-4510 cells for 48 hours with 0.144mM phenformin. (B) Graph showing the relative LC3-II protein level

adjusted with α-tubulin. (C) Graph showing the ratio of relative densities of LC3-II and LC3-I proteins.

According to the band acquired for α-tubulin it appears that a smaller amount of protein was loaded for the phenformin + galangin sample, the relative densities of LC3-I and LC3-II were adjusted accordingly.

Based on the comparison of relative densities of LC3-II on Figure 12B, it appears that phenfomin treated samples showed a small increase compared to control, whereas in cells treated with galangin the increase in LC3-II density was more than two-fold. Interestingly the combination of phenformin and galangin treatment resulted in 1.6 times increase compared to control, which is lower than the LC3-II density observed when cells were treated with galangin alone.

Relative density of a ratio of LC3-II to LC3-I was found to be highest in phenformin and galangin treated group and lowest in cells treated with phenformin alone. It showed a small increase in galangin only treated cells.

CHAPTER 4. DISCUSSION

The DoTc-4510 is a cervical cancer cell line which was found to be the most sensitive to antiproliferative effects of phenformin, as illustrated from the MTT assay data. Cervical cancer is the fourth most common cancer diagnosed in females (incidence rate of 6.6%) as well as the fourth cause of cancer-related mortality (7.5%) in females based on global statistics data acquired from 186 countries worldwide (Bray et al., 2018). Vast majority of the cervical cancer cases (99.7%) are caused by human papillomavirus (HPV) infection (Okunade, 2020). E5 is an HPV related oncoprotein that interferes with RTK pathways to result in cellular transformation, it was found to decrease LC3-II levels and reduce degradation of p62 leading to inhibition of autophagy although its precise mechanism of action is largely unknown (Lagunas-Martínez et al., 2022). A recent study by Yoo et al. (2023) found that treatment of HeLa and CaSki cervical cancer cell lines with an autophagy inducer (rapamycin) and radiation led to an increase in cell death compared to cells treated with radiation only.

Since it was previously established that mTOR has an inhibitory activity on autophagy (Li et al., 2020), it was expected that with an increased activation of autophagy the mTOR expression level will decrease. However, according to the present results shown on Figure 12B application of phenformin, galangin and a combination of these two drugs resulted in an increase in mTOR expression three-, nine- and eight-fold compared to untreated control, respectively.

In a previous study on A498 kidney cancer cells by Zhu et al. (2018), at different concentrations ranging from 7.5 to 30 μM galangin was not found to have any effect on overall mTOR expression, however the level of expression of phosphorylated mTOR (p-mTOR) was markedly decreased. Similarly, phenformin reduced the phosphorylation of mTOR at serine 2448 in a dose-dependent manner in prostate cancer cells (Kim et al., 2023). Application of phenformin at different concentrations to T24 and UMUC3 human bladder cancer cell lines did not result in changes in overall mTOR expression, however it resulted in a decreased level of phosphorylated eukaryotic translation initiation factor 4E binding protein 1 (4E-BP1) and ribosomal protein S6 kinase beta-1 (S6K1), the downstream effectors of mTOR (Huang et al, 2018). It was also found that phenformin reduced phosphorylation of S6K1 and inhibited mTORC1 non-small cell lung cancer (NSCLC) (Jang et al., 2021).

Previous research indicates that neither phenformin nor galangin affected the overall expression of mTOR between treated and control groups, however our observations are not in agreement with these findings. There could be several reasons for such a discrepancy in observations. They could be attributed to a cell-line specific response to galangin and phenformin because previous studies involved bladder, prostate and kidney cancer cells, whereas out study involved cervical cancer cells. Most importantly, it appears that phosphorylated mTOR or its downstream targets such as 4EBP1 and S6K1 would be more suitable targets for measuring the effect of phenformin on mTOR activation. While we measured the overall expression of mTOR protein, it does not give any information regarding the level of activation of this protein and detection of downstream targets of mTOR should be an important point of consideration for future studies. Additionally, to establish the reproducibility and statistical significance of the obtained results repetition of the experiment a few more times would be recommended.

P62 is a cargo protein that binds ubiquitinated proteins and directs them to the autophagosome for further degradation (Foster and Rea, 2020). When autophagy is induced the p62 levels are decreased, whereas inhibition of autophagy is associated with an accumulation of p62 within the cell (Bjørkøy et al., 2009). We expected to observe a decrease in p62 expression in phenformin if it induced autophagy in DoTc-4510 cells. As illustrated on Figure 12C, the level of p62 decreased more than two-fold in cells treated with phenformin compared to control, which may indicate the autophagy-inducing property of phenformin.

In a previous study, treatment of human glioblastoma multiforme cells with 150 μM galangin resulted in a statistically significant decrease in the level of p62 (Kong et al, 2019). In our results, however, the decrease in p62 expression induced by galangin appears to be very small. This observation could be due to the fact that the concentration of galangin used in this study is 3 times smaller (50 μM) than the one used in that paper. Also, the difference in cell line-specific response to galangin and phenformin should be considered. Interestingly, when these drugs were applied in combination the expression of p62 was increased 1.7 times, which shows that together they had an inhibitory effect on autophagy despite inducting it as individual treatments. This may have occurred due to potential drug-drug interactions between galangin and phenformin. Unfortunately, there were not any studies available where a combination of galangin and phenformin were studied regarding their effect on autophagy to compare the obtained results.

LC3-II is the lipidated form of LC3-I and it is generated when LC3-I is conjugated with phosphatidylethanolamine (PE) during the formation of a pre-autophagosomal structure (PAS) as shown on Figure 1. Current studies indicate that comparison of the amount of the detected LC3-II or the LC3-II/LC3-I ratio between samples is a more appropriate method of autophagy detection than simple comparison of LC3-I and LC3-II (Mizushima & Yoshimori, 2007). If phenformin induced autophagy, we expected to see an increase in LC3-II expression compared to control.

The expression of LC3-II was increased 1.25 times in phenformin treated cells compared to control. Notably, this small increase does not necessarily mean an increase in autophagic flux has occurred, it only means that the number of autophagosomes accumulated in the cell has increased. This can happen for two reasons either the treatment inhibited the degradation of autophagosomes or stimulated their synthesis (Mizushima & Yoshimori, 2007). To establish whether phenformin treatment resulted in stimulation of autophagosome synthesis the cells have to be treated with a lysosomal protease inhibitor such as bafilomycin 1A and if further accumulation of LC3-II is evident, this would be indicative of an increase in autophagic flux. This is an important consideration for future experiments along with the need for using other methods such as flow cytometry and/or autophagy assay for further confirmation of the results.

In glioblastoma cells treated with galangin the density of LC3-II increased almost 2.5 times and when the drugs were applied in combination an increase of 1.7 times was observed. There could be some degree of antagonistic interaction between phenformin and galangin which results in a decreased LC3-II expression compared to when galangin was applied separately. It was previously found that treatment of human glioblastoma multiforme cells with 150 μM galangin resulted in an increased level of LC3B-II, indicating an increase in autophagic flux upon treatment (Kong et al, 2019). Lee et al. (2023) found that after 2 days of 2 mM phenformin treatment colon adenocarcinoma cells showed an increased expression of LC3-II, while no difference was apparent when a concentration of 0.5 mM was applied, which is 3.5 times higher than the one used in our experiment (0.14 mM).

The ratio of relative densities of LC3-II and LC3-I was smallest in phenformin compared to control, meaning that a large part of LC3-I was not converted to LC3-II. This could potentially indicate that a small increase observed in LC3-II expression in phenformin was not due to an increase in LC3-I to LC3-II conversion, but rather due to an accumulation of autophagosomes which were not digested by lysosomal proteases. On the other hand, the ratio of relative densities of

LC3 in combination treatment of phenformin and galangin was increased over 2.5 times compared to control meaning that a larger proportion of LC3-I was converted to LC3-II. This finding and an increase in LC3-II density are somewhat contradictory with results for p62 described before because in this case one marker suggests that there is a decrease in autophagosome formation, whereas another (LC3-II and LC3-II/LC3-I ratio) suggests that there was an increase. Since no studies are available on the combined effect of galangin and phenformin on autophagy, more research is necessary for evaluation of the combined effect of these two drugs as their relationship does not appear to be straightforwardly antagonistic or synergistic in terms of autophagy induction.

CONCLUSION AND RECOMMENDATIONS

The results of this research work indicate that phenformin induces a dose-dependent reduction of viability in cells of various types of cancer. Among the studies cell lines it was also found that Dotc-4510 cervical cancer cells are the most susceptible to antiproliferative effects of phenformin based on the calculated IC50 value. The present results suggest phenformin applied at 0.14 mM on DoTc-4510 cervical cancer cells could potentially have an ability to increase autophagic flux.

To better establish phenformin's effect on the mTOR pathway in the future, measurement of phosphorylated mTOR or its downstream targets such as 4EBP1 and S6K1 would be recommended. To determine the statistical significance and confidence intervals of the obtained result, repetition of the western blot multiple times is necessary. The measurements may be taken at different time points such as every 12, 24, 36 and 48 hours for better estimation of changes in autophagic proteins over time. Visualization of autophagosomes using the autophagy assay is also recommended.

References

Ahmadi-Dehlaghi, F., Mohammadi, P., Valipour, E., Pournaghi, P., Kiani, S., & Mansouri, K. (2023). Autophagy: A challengeable paradox in cancer treatment. *Cancer Medicine*, *12*(10), 11542–11569. https://doi.org/10.1002/cam4.5577

Appleyard, M. V. C. L., Murray, K. E., Coates, P. J., Wullschleger, S., Bray, S. E., Kernohan, N. M., Fleming, S., Alessi, D. R., & Thompson, A. M. (2012). Phenformin as prophylaxis and therapy in breast cancer xenografts. *British Journal of Cancer*, *106*(6), 1117–1122. https://doi.org/10.1038/bjc.2012.56

Amaravadi, R. K., Yu, D., Lum, J. J., Bui, T., Christophorou, M. A., Evan, G. I., Thomas-Tikhonenko, A., & Thompson, C. B. (2007). Autophagy inhibition enhances therapy-induced apoptosis in a Myc-induced model of lymphoma. *The Journal of Clinical Investigation*, *117*(2), 326–336. https://doi.org/10.1172/JCI28833

Ávalos, Y., Canales, J., Bravo-Sagua, R., Criollo, A., Lavandero, S., & Quest, A. F. G. (2014). Tumor Suppression and Promotion by Autophagy. BioMed Research International, 2014, 603980. https://doi.org/10.1155/2014/603980

Bjørkøy, G., Lamark, T., Pankiv, S., Øvervatn, A., Brech, A., & Johansen, T. (2009). Monitoring autophagic degradation of p62/SQSTM1. Methods in Enzymology, 452, 181–197. https://doi.org/10.1016/S0076-6879(08)03612-4

Bray, F., Ferlay, J., Soerjomataram, I., Siegel, R. L., Torre, L. A., & Jemal, A. (2018). Global cancer statistics 2018: GLOBOCAN estimates of incidence and mortality worldwide for 36 cancers in 185 countries. *CA: A Cancer Journal for Clinicians*, *68*(6), 394–424. https://doi.org/10.3322/caac.21492

Buranaamnuay, K. (2021). The MTT assay application to measure the viability of spermatozoa: A variety of the assay protocols. Open Veterinary Journal, 11(2), 251–269. https://doi.org/10.5455/OVJ.2021.v11.i2.9

Drahota, Z., Palenickova, E., Endlicher, R., Milerova, M., Brejchova, J., Vosahlikova, M., Svoboda, P., Kazdova, L., Kalous, M., Cervinkova, Z., & Cahova, M. (2014). Biguanides inhibit complex I, II and IV of rat liver mitochondria and modify their functional properties. *Physiological Research*, *63*(1), 1–11. https://doi.org/10.33549/physiolres.932600

Foster, A. D., & Rea, S. L. (2020). The role of sequestosome 1/p62 protein in amyotrophic lateral sclerosis and frontotemporal dementia pathogenesis. Neural Regeneration Research, 15(12), 2186–2194. https://doi.org/10.4103/1673-5374.284977

García Rubiño, M. E., Carrillo, E., Ruiz Alcalá, G., Domínguez-Martín, A., A. Marchal, J., & Boulaiz, H. (2019). Phenformin as an Anticancer Agent: Challenges and Prospects. *International Journal of Molecular Sciences*, *20*(13), 3316. https://doi.org/10.3390/ijms20133316

Geoghegan, F., Chadderton, N., Farrar, G. J., Zisterer, D. M., & Porter, R. K. (2017). Direct effects of phenformin on metabolism/bioenergetics and viability of SH-SY5Y neuroblastoma cells. *Oncology Letters*, *14*(5), 6298–6306. https://doi.org/10.3892/ol.2017.6929

Guo, Z., Zhao, M., Howard, E. W., Zhao, Q., Parris, A. B., Ma, Z., & Yang, X. (2017). Phenformin inhibits growth and epithelial-mesenchymal transition of ErbB2-overexpressing breast cancer cells through targeting the IGF1R pathway. *Oncotarget*, *8*(36), 60342–60357. https://doi.org/10.18632/oncotarget.19466

Hollenstein, D. M., & Kraft, C. (2020). Autophagosomes are formed at a distinct cellular structure. Current Opinion in Cell Biology, 65, 50. https://doi.org/10.1016/j.ceb.2020.02.012

Hu, S., Ouyang, Q., Cheng, Q., Wang, J., Feng, F., Qiao, L., Gan, W., Shi, Y., Wu, D., & Jiang, X. (2018). Phenformin inhibits cell proliferation and induces cell apoptosis and autophagy in cholangiocarcinoma. *Molecular Medicine Reports*, *17*(4), 6028–6032. https://doi.org/10.3892/mmr.2018.8573

Huang, Y., Zhou, S., He, C., Deng, J., Tao, T., Su, Q., Darko, K. O., Peng, M., & Yang, X. (2018). Phenformin alone or combined with gefitinib inhibits bladder cancer via AMPK and EGFR pathways. *Cancer Communications*, *38*(1), 50. https://doi.org/10.1186/s40880-018-0319-7

Jackson, A. L., Sun, W., Kilgore, J., Guo, H., Fang, Z., Yin, Y., Jones, H. M., Gilliam, T. P., Zhou, C., & Bae-Jump, V. L. (2017). Phenformin has anti-tumorigenic effects in human ovarian cancer cells and in an orthotopic mouse model of serous ovarian cancer. *Oncotarget*, *8*(59), 100113–100127. https://doi.org/10.18632/oncotarget.22012

Jang, S.-K., Hong, S.-E., Lee, D.-H., Kim, J.-Y., Kim, J. Y., Ye, S.-K., Hong, J., Park, I.-C., & Jin, H.-O. (2021). Inhibition of mTORC1 through ATF4-induced REDD1 and Sestrin2 expression by Metformin. *BMC Cancer*, *21*(1), 803. https://doi.org/10.1186/s12885-021-08346-x

Janzer, A., German, N. J., Gonzalez-Herrera, K. N., Asara, J. M., Haigis, M. C., & Struhl, K. (2014). Metformin and phenformin deplete tricarboxylic acid cycle and glycolytic intermediates during cell transformation and NTPs in cancer stem cells. *Proceedings of the National Academy of Sciences*, *111*(29), 10574–10579. https://doi.org/10.1073/pnas.1409844111

Khandia, R., Dadar, M., Munjal, A., Dhama, K., Karthik, K., Tiwari, R., Yatoo, Mohd. I., Iqbal, H. M. N., Singh, K. P., Joshi, S. K., & Chaicumpa, W. (2019). A Comprehensive Review of Autophagy and Its Various Roles in Infectious, Non-Infectious, and Lifestyle Diseases: Current Knowledge and Prospects for Disease Prevention, Novel Drug Design, and Therapy. *Cells*, *8*(7), 674. https://doi.org/10.3390/cells8070674

Kim, Y., Yoo, S., Lim, B., Hong, J. H., Kwak, C., You, D., Hwang, J. J., & Kim, C.-S. (2023). A novel biguanide derivative, IM176, induces prostate cancer cell death by modulating the AMPK-mTOR and androgen receptor signaling pathways. *Prostate International*, *11*(2), 83–90. https://doi.org/10.1016/j.prnil.2022.11.003

Kong, Y., Feng, Z., Chen, A., Qi, Q., Han, M., Wang, S., Zhang, Y., Zhang, X., Yang, N., Wang, J., Huang, B., Zhang, Q., Xiang, G., Li, W., Zhang, D., Wang, J., & Li, X. (2019). The Natural Flavonoid Galangin Elicits Apoptosis, Pyroptosis, and Autophagy in Glioblastoma. *Frontiers in Oncology*, *9*. https://doi.org/10.3389/fonc.2019.00942

Lagunas-Martínez, A., Madrid-Marina, V., Gómez-Cerón, C., Deas, J., & Peralta-Zaragoza, O. (2022). The Autophagy Process in Cervical Carcinogenesis: Role of Non-Coding-RNAs, Molecular Mechanisms, and Therapeutic Targets. *Cells*, *11*(8), 1323. https://doi.org/10.3390/cells11081323

Lee, B., Lee, C., Moon, H.-M., Jo, S.-Y., Jang, S. J., & Suh, Y.-A. (2023). Repurposing Metabolic Inhibitors in the Treatment of Colon Adenocarcinoma Patient-Derived Models. *Cells*, *12*(24), 2859. https://doi.org/10.3390/cells12242859

Li, J., Yang, B., Zhou, Q., Wu, Y., Shang, D., Guo, Y., Song, Z., Zheng, Q., & Xiong, J. (2013). Autophagy promotes hepatocellular carcinoma cell invasion through activation of epithelial–mesenchymal transition. *Carcinogenesis*, *34*(6), 1343–1351. https://doi.org/10.1093/carcin/bgt063

Li, X., He, S., & Ma, B. (2020). Autophagy and autophagy-related proteins in cancer. Molecular Cancer, 19(1), Article 1. https://doi.org/10.1186/s12943-020-1138-4

Lim, S. M., Mohamad Hanif, E. A., & Chin, S.-F. (2021). Is targeting autophagy mechanism in cancer a good approach? The possible double-edge sword effect. *Cell & Bioscience*, *11*(1), 56. https://doi.org/10.1186/s13578-021-00570-z

Liu, Z., Ren, L., Liu, C., Xia, T., Zha, X., & Wang, S. (2015). Phenformin Induces Cell Cycle Change, Apoptosis, and Mesenchymal-Epithelial Transition and Regulates the AMPK/mTOR/p70s6k and MAPK/ERK Pathways in Breast Cancer Cells. PLoS ONE, 10(6), e0131207. https://doi.org/10.1371/journal.pone.0131207

Marsh, T., Tolani, B., & Debnath, J. (2021). The pleiotropic functions of autophagy in metastasis. *Journal of Cell Science*, *134*(2), jcs247056. https://doi.org/10.1242/jcs.247056

Miskimins, W. K., Ahn, H. J., Kim, J. Y., Ryu, S., Jung, Y.-S., & Choi, J. Y. (2014). Synergistic anti-cancer effect of phenformin and oxamate. *PloS One*, *9*(1), e85576. https://doi.org/10.1371/journal.pone.0085576

Mizushima, N., & Yoshimori, T. (2007). How to Interpret LC3 Immunoblotting. *Autophagy*, *3*(6), 542–545. https://doi.org/10.4161/auto.4600

Mowers, E. E., Sharifi, M. N., & Macleod, K. F. (2017). Autophagy in cancer metastasis. *Oncogene*, *36*(12), Article 12. https://doi.org/10.1038/onc.2016.333

Mulcahy Levy, J. M., & Thorburn, A. (2020). Autophagy in cancer: Moving from understanding mechanism to improving therapy responses in patients. *Cell Death and Differentiation*, *27*(3), 843–857. https://doi.org/10.1038/s41418-019-0474-7

Okunade, K. S. (2020). Human Papillomavirus and Cervical Cancer. *Journal of Obstetrics and Gynaecology : The Journal of the Institute of Obstetrics and Gynaecology*, *40*(5), 602–608. https://doi.org/10.1080/01443615.2019.1634030

Parzych, K. R., & Klionsky, D. J. (2014). An Overview of Autophagy: Morphology, Mechanism, and Regulation. *Antioxidants & Redox Signaling*, *20*(3), 460–473. https://doi.org/10.1089/ars.2013.5371

Pavel, M., Renna, M., Park, S. J., Menzies, F. M., Ricketts, T., Füllgrabe, J., Ashkenazi, A., Frake, R. A., Lombarte, A. C., Bento, C. F., Franze, K., & Rubinsztein, D. C. (2018). Contact

inhibition controls cell survival and proliferation via YAP/TAZ-autophagy axis. *Nature Communications*, *9*(1), Article 1. https://doi.org/10.1038/s41467-018-05388-x

Peng, Q., Qin, J., Zhang, Y., Cheng, X., Wang, X., Lu, W., Xie, X., & Zhang, S. (2017). Autophagy maintains the stemness of ovarian cancer stem cells by FOXA2. *Journal of Experimental & Clinical Cancer Research*, *36*(1), 171. https://doi.org/10.1186/s13046-017-0644-8

Rajalingam, K., Schreck, R., Rapp, U. R., & Albert, Š. (2007). Ras oncogenes and their downstream targets. *Biochimica et Biophysica Acta (BBA) - Molecular Cell Research*, *1773*(8), 1177–1195. https://doi.org/10.1016/j.bbamcr.2007.01.012

Safe, S., Nair, V., & Karki, K. (2018). Metformin-induced anticancer activities: Recent insights. *Biological Chemistry*, *399*(4), 321–335. https://doi.org/10.1515/hsz-2017-0271

Thomas, H. E., Zhang, Y., Stefely, J. A., Veiga, S. R., Thomas, G., Kozma, S. C., & Mercer, C. A. (2018). Mitochondrial Complex I Activity Is Required for Maximal Autophagy. *Cell Reports*, *24*(9), 2404. https://doi.org/10.1016/j.celrep.2018.07.101

Tonkin-Reeves, A., Giuliani, C. M., & Price, J. T. (2023). Inhibition of autophagy; an opportunity for the treatment of cancer resistance. *Frontiers in Cell and Developmental Biology*, *11*. https://doi.org/10.3389/fcell.2023.1177440

Wang, H.-X., & Tang, C. (2017). Galangin suppresses human laryngeal carcinoma via modulation of caspase-3 and AKT signaling pathways. Oncology Reports, 38(2), 703–714. https://doi.org/10.3892/or.2017.5767

Yoo, J. G., Lee, Y. K., & Lee, K. H. (2023). Enhancing autophagy leads to increased cell death in radiation-treated cervical cancer cells. *Journal of Obstetrics and Gynaecology: The Journal of the Institute of Obstetrics and Gynaecology*, *43*(1), 2171281. https://doi.org/10.1080/01443615.2023.2171281

Yun, C. W., & Lee, S. H. (2018). The Roles of Autophagy in Cancer. *International Journal of Molecular Sciences*, *19*(11), 3466. https://doi.org/10.3390/ijms19113466

Zhu, Y., Rao, Q., Zhang, X., & Zhou, X. (2018). Galangin induced antitumor effects in human kidney tumor cells mediated via mitochondrial mediated apoptosis, inhibition of cell migration and invasion and targeting PI3K/ AKT/mTOR signaling pathway.

Appendix

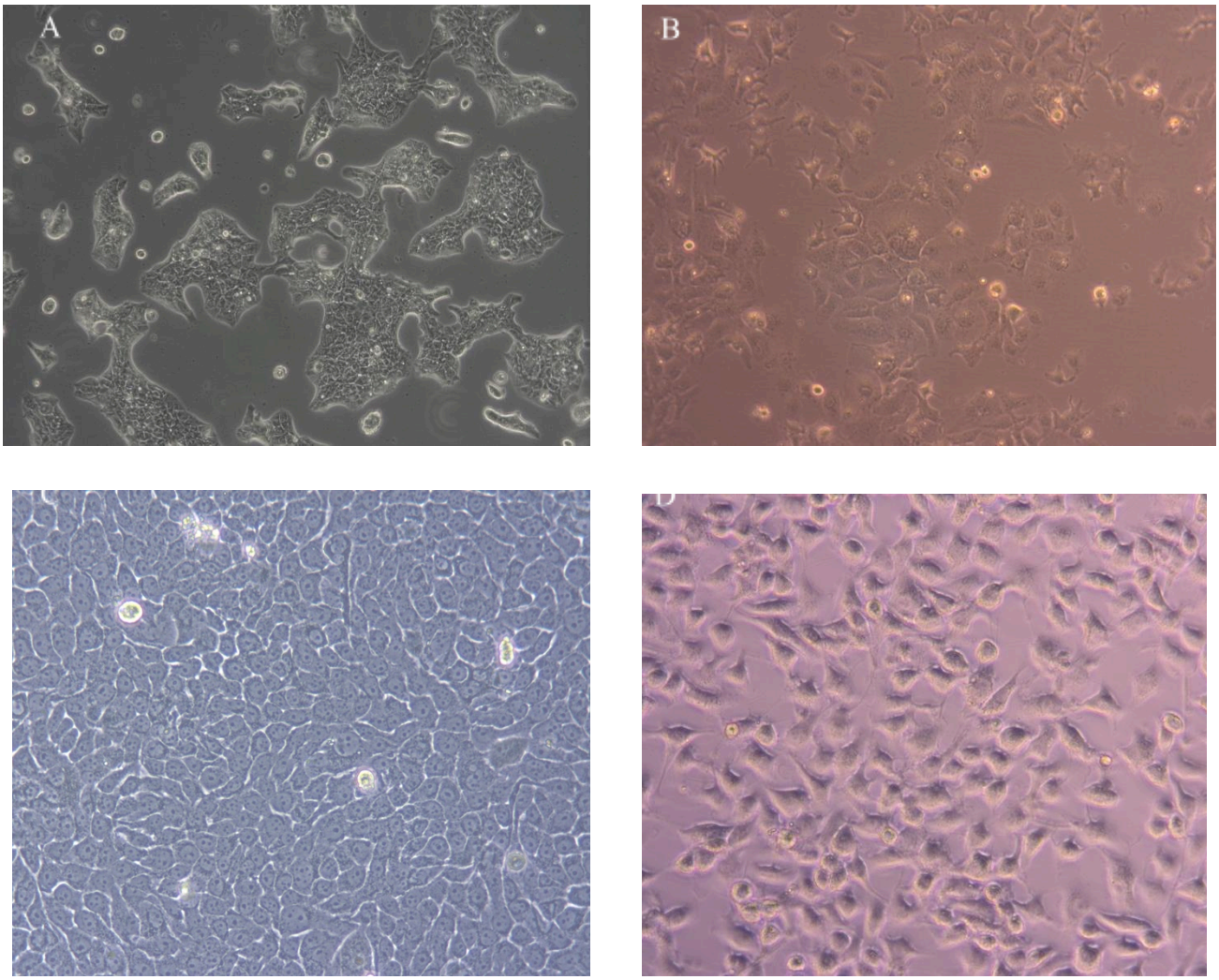

Figure 1S. Cells cultured in T25 flasks prior to seeding for the MTT assay

(A) DoTc-4510 cervical cancer cells. (B) HUH7 hepatocellular carcinoma cells. (C) Capan-2 pancreatic cancer cells. (D) MCF10 healthy breast epithelium cells.

Microscope images of other cell lines (A375, HS 578T and MCF7) used in this study could not be retrieved.

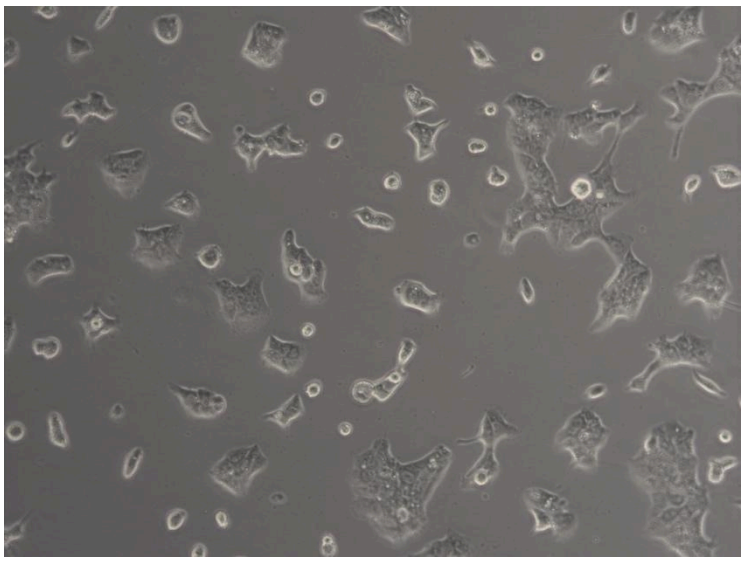

Figure 2S. DoTc-4510 cells seeded in 6-well plate prior to treatment.

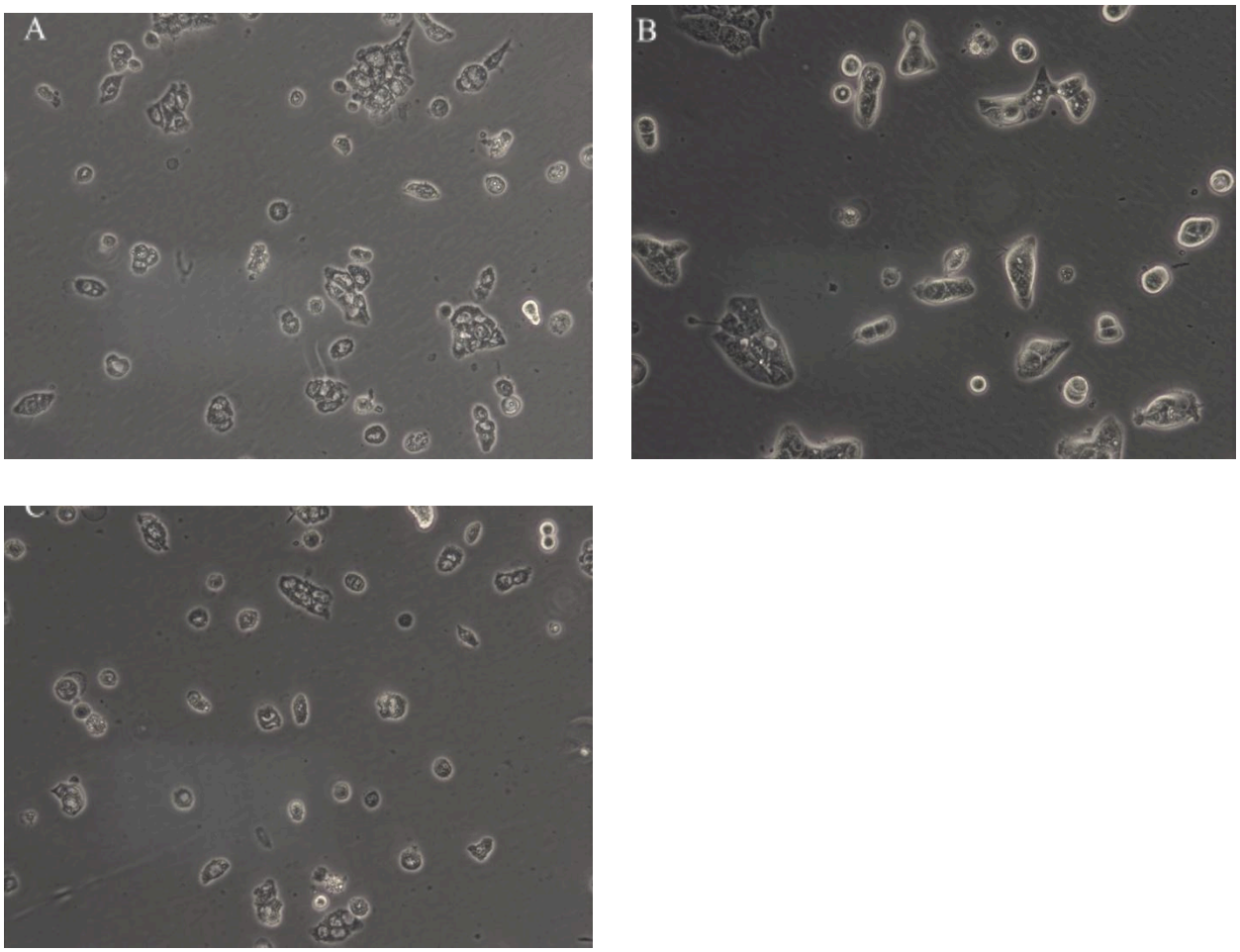

Figure 3S. DoTc-4510 cells 48 hours after treatment

(A) Untreated control. (B) Phenformin 0.14mM. (C) Phenformin 0.14mM + Galangin 50 μM.

Microscope images of galangin treatment alone could not be retrieved.

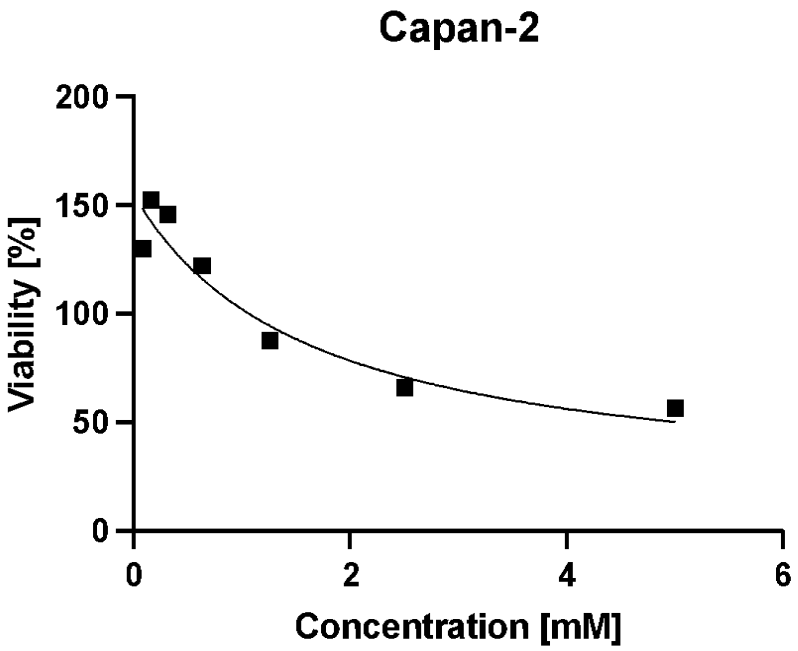

Figure 4S. Cell viability graph of Capan-2 pancreatic cancer cell line with metformin applied at different concentrations (0.0068–5 mM).

Similarly to phenformin, it appears that at 4 smallest concentrations of 0.185mM, 0.0617mM, 0.0206mM and 0.0068mM metformin has pro-proliferative effect. These results were obtained from analysis of MTT assay conducted on a single 96-well plate.